

ACCEPTED MANUSCRIPT

This is an early electronic version of an as-received manuscript that has been accepted for publication in the Journal of the Serbian Chemical Society but has not yet been subjected to the editing process and publishing procedure applied by the JSCS Editorial Office.

Please cite this article as Y. Chimbilima, M. Dadi, and T. Ahmad, *J. Serb. Chem. Soc.* (2026) <https://doi.org/10.2298/JSC250603010C>

This “raw” version of the manuscript is being provided to the authors and readers for their technical service. It must be stressed that the manuscript still has to be subjected to copyediting, typesetting, English grammar and syntax corrections, professional editing and authors’ review of the galley proof before it is published in its final form. Please note that during these publishing processes, many errors may emerge which could affect the final content of the manuscript and all legal disclaimers applied according to the policies of the Journal.



J. Serb. Chem. Soc. **00(0)** 1-20 (2026)
JSCS-13407

Adsorption of copper ions onto acid-modified *Aframomum africanum* shell: Isotherm and kinetic studies

YANE CHIMBILIMA, MURALI DADI AND TANWEER AHMAD*

Department of Chemistry, School of Mathematics and Natural Sciences, The Copperbelt University, P.O.Box.No.21692, Kitwe, Zambia.

(Received 3 June 2025; revised 29 July 2025; accepted 23 February 2026)

Abstract: In this work, copper ions have been successfully removed from aqueous solution using the acid-modified *Aframomum africanum* shell (MAAS) as an adsorbent. The adsorbent was characterized using Fourier transform infrared (FTIR) spectroscopy and field emission scanning electron microscopy (FESEM). The *afmomum africanum* shells were also characterized before and after being modified with the acid to determine their pH at the point of zero charge (pHpzc). The MAAS was found to have the pHpzc of 4.77. In batch experiments, the adsorption capacity of MAAS was investigated as a function of pH of solution, adsorbent dosage, contact time, initial copper ion concentration and agitation speed. The results revealed that at pH solution of 9, adsorbent dosage of 5 g/L, contact time of 30 min, initial Cu(II) ion concentration of 50 mg/L and at an agitation speed of 250 rpm, the maximum Cu(II) ion adsorption capacity of MAAS was 31.25 mg/g. The adsorption kinetic data and the isotherm data were also studied to find the suitable models of Cu(II) removal. The kinetic data and the isotherm data of Cu(II) removal by MAAS was found to follow the pseudo-second order kinetics model ($R^2 = 0.999$) and the Langmuir isotherm model ($R^2 = 0.990$), respectively. Therefore, the outcome suggested that the shells of *Aframomum africanum* can be utilized as an economical and efficient adsorbent to eliminate Cu(II) from aqueous solution.

Keywords: adsorption; *Aframomum africanum*; copper ion; heavy metal; adsorption kinetics; adsorption isotherms.

INTRODUCTION

The existence of life on this planet depends on the availability of water. Water is increasingly being contaminated anthropogenically with activities such as industrial activities, agriculture, poor land usage, urbanization, and non-sustainable growth. These factors have led to rapid degradation of surface and

* Corresponding author. E-mail: tanweerakhan@gmail.com
<https://doi.org/10.2298/JSC250603010C>

ground water quality.¹ Among these activities, the release of effluents containing heavy metals remains a serious concern especially for the human beings and aquatic life in mining areas of the world. According to the Environmental Protection Agency (EPA), a heavy metal is one which has a higher density and potential toxicity even at a lower concentration.² By specifying the lower limit value of heavy metals, defines heavy metals as metals having density greater than 5 g/cm³.³ A common heavy metal, copper is employed in innovative applications including solar cells and phytotherapies, as well as in decorative work and electric cable manufacturing. The element is an essential micronutrient for various processes such as photosynthesis, metabolism, and reproduction processes in living organisms.⁴ However, high concentrations of the non-biodegradable heavy metals, such as copper, in water bodies and in the soil have toxic effects on living organisms including humans.⁵ If humans are exposed to large doses of copper, degeneration or possibly necrosis of the kidneys, liver, and gastrointestinal tract would be the outcome. Copper has also been linked to changes in the nervous system or mental health issues including anxiety or insomnia.⁶

The physico-chemical techniques have mostly been employed in heavy metal eradication processes such as chemical precipitation, membrane-based techniques, ion exchange and electrochemical processes.⁷ However, these remediation techniques have some drawbacks, like high operational costs for metal complexes in trace concentrations, and high energy prerequisite.^{8,9} Efforts have been made to resolve these drawbacks by adopting the adsorption technique. The process of adsorption involves the migration and accumulation of dissolved molecules onto the surface and porous structure of a biomaterial. As adsorbents, activated carbons have been widely employed to remove harmful metal ions from wastewater. But owing to their high cost of production and regeneration challenges, there is now more effort being made to find adsorbent materials of low energy requirements, simplicity in operation and of course which can be regenerated.¹⁰ Examples of biomaterials which have been used before as adsorbents to eliminate heavy metals from wastewater include agricultural waste residues like groundnut shells, corn cob, rice husk and many more.¹¹ Adsorption has been found to exhibit the following advantages: cost effectiveness, high efficiency, easily accessible, minimal production of sludge, have a high adsorption capacity,¹² regeneration of adsorbent and possibility of metal recovery.¹³ Furthermore, the use of unconventional materials is being widely encouraged now owing to the fact that they possess functional groups that may bind metals.¹⁴⁻¹⁶

The shell of the *Aframomum africanum* plant is another agricultural waste that may be a very good adsorbent for metal removal. Among a diverse range of affordable adsorbents, the *Aframomum africanum* fruit shells (AAFS) were used as one of the promising, renewable, cost-effective biosorbents to eliminate Cu(II) ion from wastewater. *Aframomum africanum* is a perennial, bushy and wild-

growing plant with leafy stem that may be up to 1.5 m high. The leaves are simple, alternate and lanceolate with matured ones measuring as long as 40 cm in length and 12-15 cm wide. The plant is native to tropical African countries such as Ghana, Nigeria, Liberia and Cameroon and is an important commercial crop in east African countries such as Ethiopia. *Aframomum africanum* fruit belongs to the family of Zingiberaceae.¹⁷ It is one of the highly consumed fruits in Zambia which creates a notable environmental problem because the shells are usually thrown anyhow after the inner contents of the fruit have been eaten.¹⁸

To the best of the authors' knowledge, no studies have been done regarding the application of acid-modified *afframomum africanum* shell (MAAS) as an adsorbent for Cu(II) ion removal from aqueous solution. Therefore, this study was planned to assess the adsorption properties of the acid-modified *afframomum africanum* shell towards the removal of Cu(II) ions from aqueous solution. The surface functional groups and the morphology of the acid-modified *Aframomum africanum* shells were evaluated pre- and post-adsorption procedures. The experimental variables have been examined in relation to the removal of Cu (II), including the pH solution, initial metal concentration, particle size, and contact time. Analysis of the experimental data has been done using kinetic and equilibrium isotherm models.

EXPERIMENTAL

Materials

Analytical grade chemicals were used. Copper (II) sulfate pentahydrate ($\text{CuSO}_4 \cdot 5\text{H}_2\text{O}$) was prepared by dissolving in distilled water for the experiment. The solution pH was adjusted from 2 to 12 using 0.1 M sodium hydroxide (NaOH) and 0.1 M hydrochloric acid (HCl). 0.5 M Nitric acid (70%, HNO_3) was utilized for the chemical treatment of the adsorbent.

Preparation of the adsorbent

The adsorbent *Aframomum africanum* fruit shell (AAFS) was procured from Chisokone market in Kitwe town of Zambia. The authenticity of the fruit was confirmed by the department of Forest Herbarium Section under the Ministry of Green economy in Kitwe Town. The fruit shell was washed thoroughly to remove dust and impurities using tap water. Later the shells were sun-dried for 10 days and then oven-dried for 24 h at 80°C to remove the moisture from the shells properly. Dried shells were crushed in a blender and sieved by allowing the particles to pass through the 212-micrometer sieve. The powder obtained was again boiled in distilled water for 24 h to completely eliminate any coloration from the sample. Finally, the sample was dried in the oven for 24 h at 80°C to remove the moisture and stored in an air-tight bottle.

Chemical modification of the AAFS dried powder

The AAFS dried powder (82.58 g) was added to a 2 L conical flask that contained 0.5 M dilute nitric acid. The mixture was shaken for 2 h on the orbital shaker at 140 rpm and was left to stand for 24 h. After repeatedly washing the modified sample in distilled water to get rid of any remaining nitric acid, it was dried in an oven set at 60°C for 48 h. The modified AAFS powder (now called MAAS) was stored in an air-tight bottle for later use. The flow diagram of

Aframomum africanum fruit shell drying and its conversion into acid-modified adsorbent is shown in Fig. 1.



Fig.1. Schematic representation of *Aframomum africanum* fruit shell drying and its conversion into acid-modified adsorbent

Preparation of copper sulfate solution

To prepare a 1000 ppm Cu (II) sulphate stock solution, 3.93 g of copper (II) sulphate pentahydrate ($\text{CuSO}_4 \cdot 5\text{H}_2\text{O}$) was dissolved in a litre of distilled water. All subsequent Cu(II) ion concentration solutions in this experiment were prepared by withdrawing the calculated volume of stock solution and diluting it in a required volume standard flask using distilled water only. To prepare a solution of a specific concentration, dilution formula was used.

Characterization of the adsorbent

The different functional groups on the adsorbent's surface were identified using the Fourier Transform Infrared (Alpha-II, Bruker, Germany). With a resolution range of $2\text{--}4\text{ cm}^{-1}$, the FTIR spectra were captured before and after the Cu(II) adsorption within the wave number $400\text{--}4000\text{ cm}^{-1}$ region. The FESEM (JEOL-JST-IT80, Japan) was used to investigate the surface morphology of the adsorbent before and after the adsorption processes.

The pH_{PZC} parameter was determined by placing 40 ml of an aliquot of sodium nitrate in 10 different Erlenmeyer flasks. The pH of the sodium nitrate solutions in the Erlenmeyer flasks was changed from 3 to 12 by reading values on the pH meter using 0.1 M HCl and 0.1 M NaOH solutions. To each flask 5 g of the adsorbent was added and the flasks taken on the shaker to be shaken for 24 h. After equilibrium, the content was filtered, the final pH of the filtrate of each

flask measured and recorded. Finally, plots of change in pH (ΔpH , i.e. initial pH – final pH) against initial pH (pH_i) were put on a graph.

Batch adsorption studies

In the batch experiment, 250 mL conical flasks were used to pour 100 mL Cu(II) solution with the calculated amount of MAAS adsorbent. To get the concentration needed for each experiment, the Cu(II) solution was diluted with distilled water in a standard flask. The content of the conical flask was then agitated at a fixed number of revolutions per minute on a shaker, for a fixed contact time and at room temperature. After that, filter paper was used to separate the adsorbent from the mixture. The residual concentrations of Cu ions were measured using an Atomic Absorption spectrophotometer (contraAA 300, Analytik Jena, Germany.)

The adsorption capacity (amount of adsorption) of the adsorbent at equilibrium, q_e (mg/g), and the percentage of heavy metal removal $R(\%)$ were determined using the equations stated below.

$$q_e = \frac{C_i - C_e}{m} \times V \quad (1)$$

$$R(\%) = \frac{C_i - C_e}{C_i} \times 100 \quad (2)$$

where m is the dry weight of the adsorbent (g), V is the volume of the Cu(II) ions in solution(L), C_i is the initial Cu(II) ion concentration (mg/L), C_e is the Cu(II) ion concentration (mg/L) at equilibrium, and q_e is the adsorption capacity (mg/g) of MAAS at equilibrium.

The effect of independent variables, such as contact time (5 min to 120 min), and initial Cu(II) concentration (10 mg/L to 150 mg/L) on the adsorption capacity of MAAS adsorbent against Cu(II) was observed at a fixed temperature (25° C), fixed volume of Cu(II) solution (100 mL) and adsorbent dosage (5.0 g/L). The effect of varying each individual parameter was investigated while holding the other parameters constant. To calculate for the kinetic parameters, the adsorption data of Cu(II) against time was exploited and in order to calculate for the isotherm parameters, the adsorption data of Cu(II) against its equilibrium concentration was equally exploited. Additionally, regression coefficients (R^2) were calculated for the adsorption kinetics and the isotherms.

RESULTS AND DISCUSSION

FTIR analysis of the MAAS

It is crucial to identify the chemical functional groups on the adsorbent's surface in order to understand the adsorption mechanism of Cu(II) by the adsorbent. The chemical functional groups present could be responsible for the metal ion binding onto the surface of the adsorbent.¹⁹ As seen in Fig. 2 below, the FTIR spectrum of MAAS before adsorption contains hydroxyl groups (-O-H) and phenols as well as the -N-H group indicated by the broad transmission peak at 3365.²⁰ The asymmetric C-H stretching of surface methyl groups, which are often found on the lignin structure, is indicated by the peak at 2917 cm^{-1} .^{21,22} The band observed around 1637 cm^{-1} is due to the C=O stretching in carbonyl group. The C-O stretching of alcohol and carboxylic acid in cellulose, hemicelluloses, and lignin, or C-O-C stretching in cellulose and hemicellulose, was identified by the strong band at 1043 cm^{-1} .²⁰ The role played by these functional groups is quite

important in heavy metal adsorption because of the functional groups' affinity for the metal ions.

The FTIR spectrum of post adsorption MAAS (MAAS -Cu) is shown in Fig.2 as well. It was observed that the post adsorption spectra were having peak at exactly the same wave number as pre-adsorption spectra. However, the difference in the reduction of peak intensities was observed. The reduction in peak intensities suggests the involvement of various functional groups in complexation with Cu(II) without undergoing major chemical transformation. Additionally, this showed that the copper adsorption mechanism involved a large number of the functional groups found in the spectra.⁹

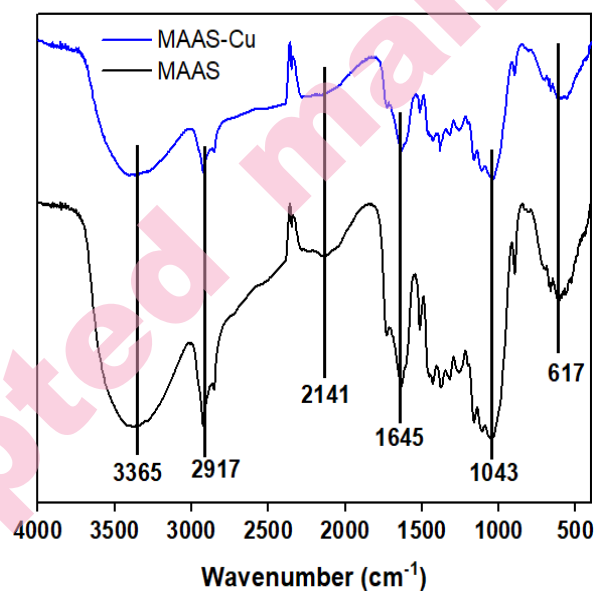


Fig. 2. FT-IR spectra for the acid-treated adsorbent

FESEM analysis of MAAS

Using the FESEM, the surface morphology of MAAS was analyzed before and after the adsorption of Cu(II) ion. Fig. 3 (a) shows the surface morphology of the adsorbent before Cu(II) adsorption while Fig. 3 (b) represents the Cu(II) adsorbed onto the surface of MAAS.

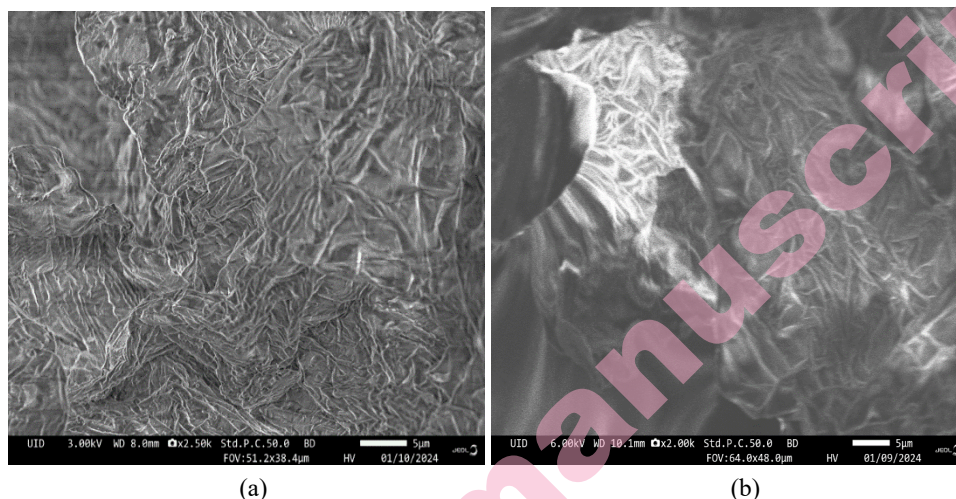


Fig. 3FESEM images of MAAS (a) before adsorption of Cu(II) and (b) after adsorption of Cu(II).

Pre-adsorption surface of MAAS (Fig. 3. (a)) is having the pores and cavities on the rough and uneven surface of the acid-modified adsorbent. The post-adsorption MAAS surface pores were covered with Cu(II) ions, as seen in Fig. 3.(b), and the majority of the pores are now invisible. Furthermore, the post-adsorption MAAS surface became somewhat smoother. It indicated that the surface pores were covered with Cu(II) ions.

Point of zero charge

It is the pH at which the adsorbent surface has no net charge. The pH_{PZC} of MAAS was determined for both the untreated adsorbent and the nitric acid-treated adsorbent. The results are shown in Fig.4. The acid-modified adsorbent had a pH_{PZC} of 4.77, which means that at pH lower than this its surface is positively charged and at pH higher than 4.77 the adsorbent's surface is negatively charged. The pH_{PZC} of untreated adsorbent was 7.62.

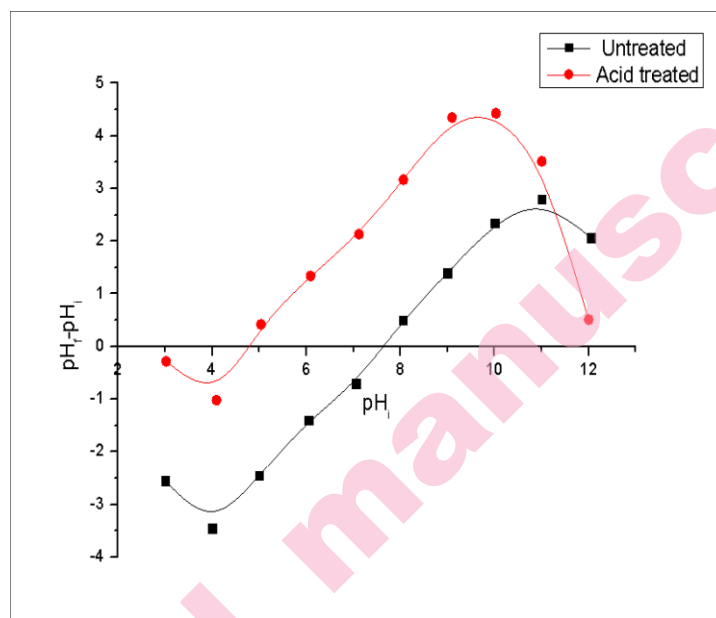


Fig. 4 pHzpc of the untreated and the treated adsorbent

Effect of solution pH

The most significant parameter affecting the adsorption of Cu(II) ions onto MAAS is solution pH. It establishes the adsorbent's surface charge as well as the adsorbate's degree of ionization and speciation.²³ The pH of the Cu(II) solutions was changed from 2 to 12 while maintaining the same initial concentration of 50 mg/L, contact time of 60 min, agitation speed of 150 rpm, and dosage of 5 g/L. From the experiment, maximum adsorption was 99.73 % at pH 9. The percentage of copper removed was low at low pH. The adsorbent surface is positively charged if the pH of the solution is lower than pHzpc. Conversely, for a solution pH greater than pHzpc, deprotonation causes the adsorbent surface to become negatively charged, which promotes Cu(II) and the adsorbent surface's electrostatic attraction and raises the adsorption percentage.⁹ This is explained by the extra H⁺ that surrounds the binding sites and causes a protonation process that makes them positively charged. This results in the repulsion of metal cations away from the adsorption sites making the adsorption process unfavorable. Additionally, the presence of H⁺ ions in solution results in competitive adsorption between the H⁺ and the metal cations. This leads to competition between H⁺ and Cu(II) for the adsorbent's adsorption sites, which results in repulsion.^{24, 25} Thus, the pH 9 of the solutions was chosen which is a pH beyond PZC for the follow-up adsorption studies. Above pH 9 the percentage removal of Cu(II) decreased. This may be due to the hindrance effect caused by the abundant OH⁻ ions (hydroxide precipitation)

preventing the diffusion of Cu(II) to the adsorbent. The results are shown in the Fig. 5(a).

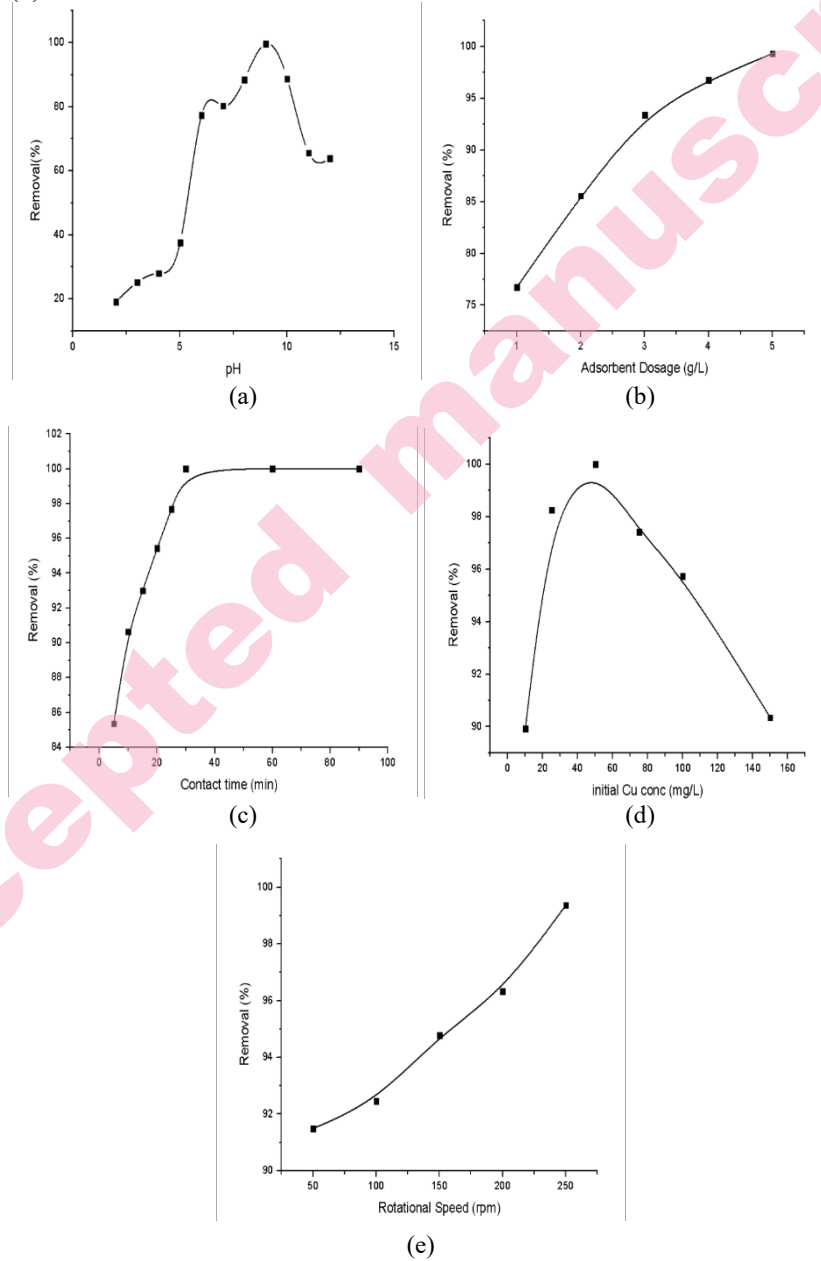


Fig. 5 Effect of (a) solution pH (b) adsorbent dosage (c) contact time (d) initial Cu(II) concentration (e) Rotational speed

Effect of adsorbent dose

To explore the influence of adsorbent dosage on the elimination of copper from wastewater, the dosage was varied for values of 0.5, 1.0, 2.0, 3.0, 4.0 and 5.0 g/L while keeping other parameters unchanged (pH 9, contact time 60 min, initial concentration 50 mg/L and agitation speed 150 rpm). The results in Fig. 5(b) show that the removal efficiency went up with increasing adsorbent dosage producing the highest efficiency removal of 99.33% at a dosage of 5 g/L. The increased percentage removal can be attributed to the number of available adsorption sites which increased with the mass of the adsorbent.²⁶ Therefore, an optimal adsorbent dosage of 5 g/L was used in the follow-up adsorption experiments.

Effect of contact time

The time of contact between the adsorbent and the aqueous metal solution is another parameter which influences the uptake of metal ions. At constant parameters (pH 9, adsorbent dose 5 g/L, initial concentration 50 mg/L and agitation speed 150 rpm), studying the effect of contact time (5, 10, 20, 30, 60, 90, 120 min) on the removal percentage of Cu(II), the results are revealed in Fig. 5(c). From the graph, the greatest removal efficiency of Cu(II) was more pronounced during the first 30 min. This is attributed to the availability of vacant sorption sites of the adsorbent during the initial stage of the adsorption process.²⁷ After 30 min, the amount of Cu(II) adsorbed remained unchanged. This could be as a result of the active sites present on the adsorbent's surface being saturated by the Cu (II) molecules.

Effect of initial Cu(II) concentration

The effect of initial Cu(II) concentration on the removal efficiency was investigated for different solution concentrations of 10, 25, 50, 75, 100 and 150 mg/L while ensuring that the other parameters were kept constant. From the experimental results, the percentage removal of Cu(II) increased with the increase of Cu(II) concentration from 10 mg/L to 50 mg/L. As can be seen from Fig. 5(d), the removal efficiency increased from 89.93 % for the initial Cu(II) concentration of 10 mg/L to 100 % for the initial Cu(II) concentration of 50 mg/L after the adsorption process. However, from 50 mg/L, further increase in the initial Cu(II) concentration resulted in a decreased efficiency removal by the adsorbent. This reduced removal at higher initial concentrations is attributed to the adsorbent's surface being saturated at the relatively high metal concentration¹³ and also desorption started to occur.²⁸

Effect of agitation speed

The influence of varying the speed of agitation at 50, 100, 150, 200 and 250 rpm was also investigated while maintaining other parameters constant (pH 9, adsorbent dose 5g/L, 30 min of contact time and initial metal concentration 50 mg/L). From the experimental results obtained in Fig. 5(e), the removal efficiency

increased with an increase in the speed of agitation. The results show a maximum removal percentage of almost 100 % at an agitation speed of 250 rpm. At low speeds the adsorbent accumulates at the bottom instead of spreading throughout the solution. The result is that the sorption sites below the above layers of the adsorbent get buried leading to the low removal percentage of the metal ions. Therefore, the speed of agitation of the adsorbate-adsorbent mixture should be sufficient enough to ensure the adsorbent spreads throughout the solution so that the unoccupied binding sites are exposed for the metal uptake.²⁹

Adsorption isotherm studies

In order to investigate the distribution of Cu(II) ions between the adsorbent and the bulk solution, the most common adsorption isotherm models were used by fitting the equilibrium adsorption data into their respective isotherm equations.³⁰ The adsorption isotherm models used were the Langmuir, Freundlich, Temkin and Dubinin-Radushkevich (D-R) isotherm models.

Langmuir adsorption isotherm

The Langmuir adsorption isotherm model suggests that the adsorption of adsorbate molecules onto the adsorbent surface is monolayer,³¹ and that the adsorbent has a finite number of homogeneously distributed and energetically uniform sorption sites. Therefore, this model applies to adsorption on adsorbent surfaces which are entirely homogeneous. The Langmuir isotherm in linear form is defined by:

$$\frac{C_e}{q_e} = \frac{1}{q_m \times K_L} + \frac{1}{q_m} \times C_e \quad (3)$$

Where C_e is the equilibrium concentration of adsorbate (mg/L), q_e is equilibrium adsorption capacity (mg/g), q_m is the Langmuir adsorption constant related to maximum adsorption capacity (mg/g), K_L is also the Langmuir adsorption constant (L/mg) related to sorption energy.

A plot of C_e/q_e vs C_e should yield a straight line if the Langmuir isotherm model is obeyed by the adsorption equilibrium as shown in Fig. 6(a). From the plot, we can evaluate the values of q_m and K_L which are obtained from the slope ($1/q_m$) and the intercept ($1/q_m K_L$) respectively.

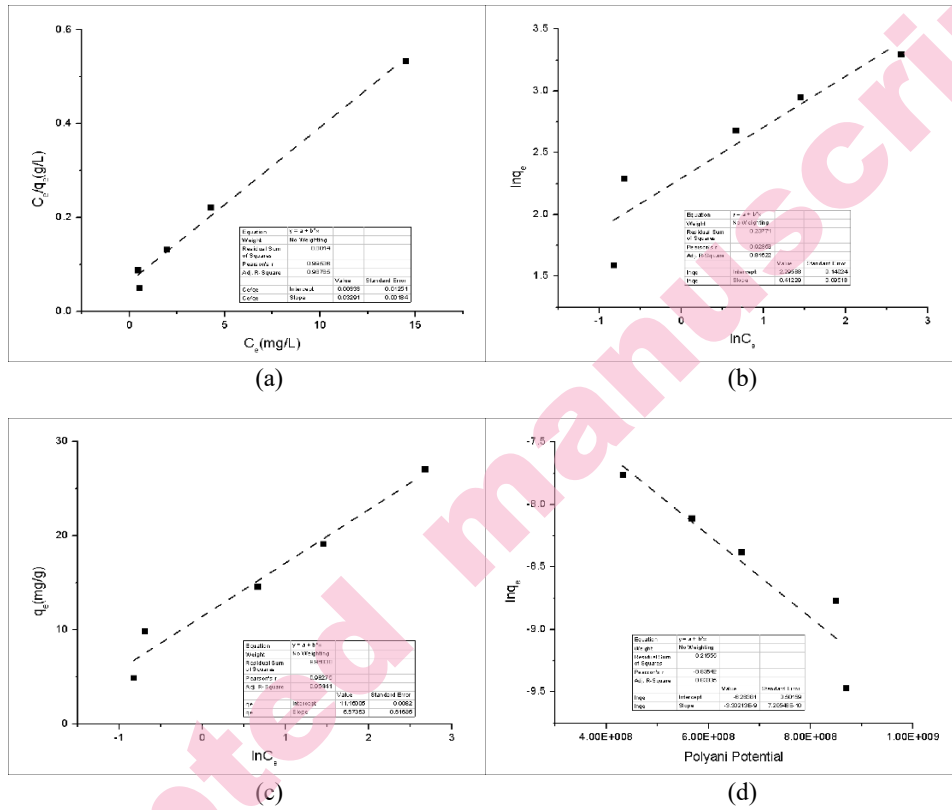


Fig. 6 Adsorption isotherm plots of Cu(II) removal through MAAS (a) Langmuir linear model (b) Freundlich linear model plot, (c) Temkin isotherm linear model plot, and (d) D-R isotherm linear model.

An important aspect of the Langmuir isotherm called the separation factor, R_L , (a dimensionless constant) is very useful in predicting affinity between adsorbate and adsorbent.³² The separation factor which is also called the equilibrium parameter is defined by

$$R_L = \frac{1}{1 + K_L \times C_i} \quad (4)$$

Where, K_L is the Langmuir isotherm constant (L/mg) and C_i is the initial metal ion concentration (mg/L). By determining the magnitude of the separation factor, the adsorption process is favorable within the range $0 < R_L < 1$, unfavorable when $R_L > 1$, becomes linear when $R_L = 1$, and the process is irreversible when $R_L = 0$. The Langmuir constant ($K_L = 0.508$) indicates a strong affinity between adsorbent and adsorbate. Furthermore, the separation factor ($R_L = 0.04$), being closer to zero confirms highly favorable adsorption. Table I shows that adsorption follows Langmuir isotherm model ($R^2 = 0.99$) with q_{max} of 31.25 mg/g. Modified

Aframomum africanum shell have a higher biosorption capacity for Cu(II) ion removal than most of the biosorbents previously described in the literature.³³⁻³⁶

Freundlich adsorption isotherm

Freundlich adsorption isotherm suggests that the uptake of adsorbate solutes occurs on the heterogeneous surface of an adsorbent by multilayer adsorption. The model's assumption is that the uptake of sorbate molecules occurs on the heterogeneous surface of an adsorbent by multilayer adsorption.³⁷ This isotherm model describes adsorbents whose active sites have different affinities or adsorption energies for adsorbate solutes. The Freundlich isotherm model in linear form is defined by:

$$\ln q_e = \ln k_F + \frac{1}{n} \ln C_e \quad (5)$$

Here, q_e is the amount of adsorbate molecules adsorbed per unit mass of adsorbent (mg/g), K_F is the measure of adsorption capacity (mg/g), n is related to the adsorption intensity (affinity) (no unit) and C_e is the concentration of metal ions at equilibrium (mg/L). The values of the Freundlich constants can be obtained by plotting a graph of $\ln q_e$ vs $\ln C_e$ with $\log k_F$ as the intercept and the slope equal to $1/n$ shown in Fig. 6(b). The magnitude of n indicates the favorability of biosorption. If the value of $n < 1$ then the biosorption is unfavorable, when $n = 1$ then the separation within the two phases is not dependent on the concentration and when $n > 1$, it implies the adsorption of the adsorbate molecules onto the adsorbent surface is favorable. The Freundlich constant ($K_F = 9.92$) indicates a high adsorption capacity of the adsorbent. The value of $1/n = 0.412$ ($n = 2.43$) suggests favorable adsorption on a heterogeneous surface. However, the comparatively lower R^2 value indicates that the Freundlich isotherm provides a weaker fit than the Langmuir isotherm. The value of n and K_F calculated using slope and intercept were 2.42 and 9.92 with $R^2 = 0.862$ as shown in Table I. Consequently, adsorption has been conducted as a chemical process since the value of $n > 1$.

Temkin adsorption isotherm

The heat involved in the adsorption of Cu(II) on MAAS was evaluated through Temkin isotherm. It is assumed that the decline in the heat of adsorption followed a linear trend as opposed to a logarithmic curve.³⁸ The following equation represents the Temkin isotherm in its non-linearized form (Eq. (9)).

$$q_e = \frac{RT}{b} \ln K_T + \frac{RT}{b} \ln C_e \quad (6)$$

$$B = \frac{RT}{b} \quad (7)$$

where B , which deals with the heat generated during adsorption, is constant. As illustrated in Fig. 6(c), the slope of the q_e vs. $\ln C_e$ plot can be used to compute the heat of adsorption constant (b). The Temkin constant b (436.73 J/mol) indicates

a moderate heat of adsorption, suggesting that the process is predominantly physical in nature. The equilibrium binding constant ($K_T = 7.52$ L/mg) reflects a good affinity between the adsorbent and adsorbate. Table I provide a summary of the computed values for the Temkin isotherm constants and associated parameters. The computed values are close to the actual heat involved in the adsorption, as indicated by the model's correlation coefficient for Cu(II) adsorption data, which was determined to be 0.985.

Dubinin-Radushkevich (D-R) adsorption isotherm

The Dubinin-Radushkevich isotherm assumes that the sorption sites are not identical and takes into account the idea of adsorbent surface heterogeneity, just like the Freundlich isotherm does.³⁹ The D-R model's linearized form is provided below:

$$\ln q_e = \ln q_{2max} \quad (8)$$

where ε (kJ^2mol^2) is the Polanyi potential and β (mol^2/J^2) is the activity coefficient associated with mean adsorption energy.

The following relation in equation (9) was used to derive the Polanyi potential⁴⁰ (ε).

$$\varepsilon = RT \ln\left(1 + \frac{1}{C_e}\right) \quad (9)$$

The mean free energy of adsorption (E_A) per molecule of adsorbate can be calculated using the Dubinin-Radushkevich isotherm constant (K_{D-R}) when the adsorbate molecules migrate from infinity to the adsorbent surface. It can be computed using the equation below Eq. (10).

$$E_A = \frac{1}{\sqrt{2K_{D-R}}} \quad (10)$$

Table I lists the Dubinin-Radushkevich isotherm constants for Cu(II) adsorption upon MAAS along with the associated mean free energy of adsorption. The type of the adsorbent and adsorbate determines the adsorption potential, which was unaffected by temperature. It is possible to determine whether adsorption is physical or chemical ion exchange by examining the mean free energy of the adsorption (E_A). The adsorption phase that comes after the chemical ion exchange is shown by the values of E_A that fall between 8 and 16 kJ/mol. The average free energy for this adsorption ($E_A = 12.90$ kJ/mol) falls within the range, indicating that ion-exchange followed the adsorption mechanism. The D-R constant β (3.00×10^{-9} mol^2/J^2) suggests a narrow energy distribution and supports adsorption occurring predominantly in micro porous region of the adsorbent. Fig. 5(d) displays the linearized D-R plot, and the linear plot's correlation coefficient (R^2) was determined to be 0.875. As a result, the Langmuir isotherm was better suited by the adsorption data than the Freundlich, Temkin, and D-R isotherm models.

TABLE I. Adsorption isotherm models of Cu(II) adsorption onto modified *Aframomum africanum* shells

Models	Model Parameters	MAAS
	Temperature (°C)	25
Langmuir	q_{\max} (mg/g)	31.25
	K_L (L/mg)	0.508
	R_L	0.04
	R^2	0.99
Freundlich	K_F (mg.L/mg.g)	9.92
	$1/n$	0.412
	R^2	0.862
Temkin	b (J/mol)	436.73
	K_T (L/mg)	7.52
	R^2	0.985
D-R	q_{\max} (mg/g)	121.1
	q_{\max} (mmol/g)	1.91
	E (kJ/mol)	12.9
	β	3.00×10^{-9}
	R^2	0.875

Adsorption kinetic study

During adsorption studies, determining the rate and comprehending the mechanism of heavy metal adsorption are crucial. In order to fit the experimental results, various kinetic models have been presented.⁴¹ The pseudo-first-order kinetic model and the pseudo-second-order kinetic models are the only two kinetic models covered in this study.

Pseudo-first-order kinetics model

The pseudo-first-order rate equation is written as⁴²

$$\frac{dq_t}{dt} = k_1(q_e - q_t) \quad (11)$$

Where q_e and q_t (mg/g) are the amount of metal ions adsorbed per gram on the surface of adsorbent at equilibrium and at time 't', respectively, and k_1 (1/min) is the equilibrium rate constant of pseudo-first-order adsorption. Integrating equation (3) by applying conditions $t = 0$ to $t = t$ and $q_t = 0$ to q_t , the above equation becomes

$$\ln(q_e - q_t) = \ln q_e - k_1 \times t \quad (12)$$

As illustrated in Fig. 7(a), linear plots of $\log(q_e - q_t)$ versus t suggest the applicability of this kinetic model. From the graph of $\ln(q_e - q_t)$ against time t , k_1 may be computed.

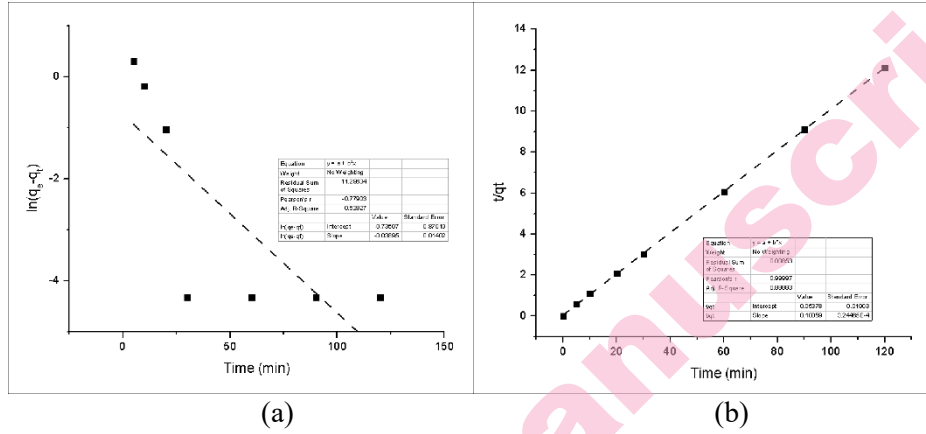


Fig. 7 Adsorption kinetic plots of Cu(II) removal (a) pseudo-first order kinetic model plot, (b) pseudo-second order kinetic model plot.

Pseudo-second-order kinetics model

The linearized pseudo-second-order form of equation is given by⁴³

$$\frac{t}{q_t} = \frac{1}{k_2 \times q_e^2} + \frac{1}{q_e} \times t \quad (13)$$

The equilibrium rate constant of the pseudo-second-order kinetics model is k_2 (g/mg/min), while q_e and q_t (mg/g) represent the quantity of metal ions adsorbed per gram on the adsorbent surface at equilibrium and at time "t," respectively. The mechanism of adsorption is assumed to follow a second-order kinetics model if a plot of t/q_t against t produces a straight-line graph. The plot's slope ($1/q_e$) and intercept ($1/k_2q_e$) yield the values of q_e and k_2 , respectively.

TABLE II. Adsorption kinetic models of Cu(II) ion adsorption by modified *Aframomum africanum* shells

Models	Model Parameters	MAASP
Pseudo-first-order	q_e (mg/g)	0.478
	k_1 (1/min)	0.038
	R^2	0.606
Pseudo-second-order	q_e (mg/g)	10
	K_2 (g/mg/min)	0.189
	R^2	0.999

A well-established kinetic models, such as pseudo-first order (PFO) and pseudo-second order (PSO) were used, to study the adsorption kinetics of Cu(II) adsorption onto MAAS. The Cu(II) adsorption data were collected at 50 mg/L initial concentration at different time intervals (from 5 min to 120 min) and applied to linearized pseudo-first order and pseudo-second-order kinetic models shown in Fig.7(a-b). Within 30 min of contact time, 99% of adsorption was found to occur.

Pseudo-first order and pseudo-second kinetic models were used to visualize the collected kinetic data. From the plotted data, it was observed that Cu(II) adsorption onto MAAS poorly followed the pseudo-first order kinetic ($R^2 = 0.606$) shown in Fig. 7(a) but perfectly followed the PSO kinetic model. The linear curve fitting of the PSO model gave the correlation coefficient (R^2) value of 0.999 shown in Fig. 7(b). It was also observed that for PSO kinetics, the theoretical adsorption capacity $q_{e, cal}$ (10.00 mg/g) and experimental values $q_{e, exp}$ (9.901 mg/g) were extremely close, however for PFO kinetics, these values were different. The PSO kinetics model was therefore more applicable, as evidenced by the same values for $q_{e, cal}$ and $q_{e, exp}$ and a higher regression coefficient value ($R^2 = 0.99$) compared to the pseudo-first-order model ($R^2 = 0.606$). Table III incorporates the R^2 value, slope and intercept of adsorption isotherms and kinetic model.

Table III. Adsorption isotherms and kinetics models parameters of Cu(II) ion adsorption onto modified *afframomum africanum* shell

Models	Parameters	Values
Langmuir Isotherm	R^2	0.990
	Slope	0.032
	Intercept	0.063
Freundlich Isotherm	R^2	0.862
	Slope	2.42
	Intercept	9.92
Temkin Isotherm	R^2	0.985
	Slope	5.67
	Intercept	11.45
D-R Isotherm	R^2	0.875
	Slope	3.30×10^{-9}
	Intercept	-6.26
Pseudo-First Order Kinetic	R^2	0.606
	Slope	-0.039
	Intercept	-0.737
Pseudo-Second Order Kinetic	R^2	0.999
	Slope	0.100
	Intercept	0.054

CONCLUSION

In the present study, low-cost adsorbents were successfully prepared from *Aframomum africanum* fruit through chemical modifications of surface. Nitric acid was used to modify the fruit shell powder, FESEM and FT-IR were used to observe the changes in adsorbent surface. The adsorption of Cu(II) from aqueous solution by the acid-modified adsorbent was investigated for various conditions of pH, adsorbent dosage, contact time, initial Cu(II) concentration and agitation speed. Among these conditions pH was found to be the most significant feature affecting the adsorption of Cu(II). For a dosage of 5 g/L, a contact time of 30 minutes, and

an initial Cu(II) concentration of 50 mg/L, the maximum removal of Cu(II) was 100% at pH 9. The Langmuir isotherm model and the pseudo-second-order model were able to adequately fit the experimental results. The Langmuir isotherm predicted monolayer adsorption of Cu(II) ions with maximum absorption capacity of 31.25 mg/g. *Aframomum africanum* is an effective adsorbent for the sequestration of Cu (II) from aqueous solution, according to the experimental data.

Acknowledgements: Thanks to Department of Chemistry, School of Mathematics and Natural Sciences, The Copperbelt University for laboratory facilities.

ИЗВОД

АДСОРПЦИЈА ЈОНА БАКРА НА КИСЕЛИНОМ МОДИФИКОВАНУ ЉУСКУ *Aframomum africanum*: ИЗОТЕРМСКА И КИНЕТИЧКА ИСПИТИВАЊА

YANE CHIMBILIMA, MURALI DADI, TANWEER AHMAD

Department of Chemistry, School of Mathematics and Natural Sciences, The Copperbelt University,
P.O.Box.No.21692, Kitwe, Zambia.

У овом раду јони бакра су успешно уклоњени из воденог раствора применом киселином модификоване љуске *Aframomum africanum* (MAAS) као адсорбента. Адсорбент је окарактерисан применом инфрацрвене спектроскопије са Фуријеовом трансформацијом (FTIR) и скенирајуће електронске микроскопије са емисијом поља (FESEM). Љуске *Aframomum africanum* су такође окарактерисане пре и после киселинске модификације ради одређивања pH вредности на тачки нултог наелектрисања (pH_{zpc}). Утврђено је да MAAS има pH_{zpc} вредност 4,77. У серији батч експеримената испитиван је адсорпциони капацитет MAAS-а у зависности од pH вредности раствора, дозе адсорбента, времена контакта, почетне концентрације јона бакра и брзине мешања. Резултати су показали да је при pH вредности раствора 9, дози адсорбента од 5 g/L, времену контакта од 30 минута, почетној концентрацији Cu(II) јона од 50 mg/L и брзини мешања од 250 rpm постигнут максимални адсорпциони капацитет MAAS-а за Cu(II) јоне од 31,25 mg/g. Кинетички подаци и подаци изотерме адсорпције анализирани су ради одређивања одговарајућих модела уклањања Cu(II). Утврђено је да кинетички подаци прате модел псеудо-другог реда ($R^2 = 0,999$), док изотермски подаци прате Ленгмиров модел изотерме ($R^2 = 0,990$). Резултати указују да се љуске *Aframomum africanum* могу користити као економичан и ефикасан адсорбент за уклањање Cu(II) јона из водених раствора.

(Примљено 3. јуна 2025; ревидирано 29. јула 2025; прихваћено 23. фебруара 2026.)

REFERENCES

1. A. Hussain, S. Madan, R. Madan, *Removal of Heavy Metals from Wastewater by Adsorption*, in *Heavy Metals - Their Environmental Impacts and Mitigation*, M. K. Nazal, H. Zhao, Ed(s), IntechOpen, 2021. (<https://doi.org/10.5772/intechopen.95841>)
2. D. Piwowarska, E. Kiedrzyńska, K. Jaszczyszyn, *Crit. Rev. Environ. Sci. Technol.* **54** (2024) 1436 (<https://doi.org/10.1080/10643389.2024.2317112>)
3. P. B. Angon, M. S. Islam, K. C. Shreejana, A. Das, N. Anjum, A. Poudel, S. A. Suchi, *Heliyon* **10** (2024) e28357 (<https://doi.org/10.1016/j.heliyon.2024.e28357>)

4. M. Rehman, L. Liu, Q. Wang, M. H. Saleem, S. Bashir, S. Ullah, D. Peng, *Environ. Sci. Pollut. Res.* **26** (2019) 18003 (<https://doi.org/10.1007/s11356-019-05073-6>)
5. S. Mitra, A. J. Chakraborty, A. M. Tareq, T. B. Emran, F. Nainu, A. Khusro, A. M. Idris, M. U. Khandaker, H. Osman, F. A. Alhumaydhi, J. Simal-Gandara, *J. King Saud Univer.– Sci.* **34** (2022) 101865. (<https://doi.org/10.1016/j.jksus.2022.101865>)
6. J. Briffa, E. Sinagra, R. Blundell, *Heliyon* **6** (2020) e04691 (<https://doi.org/10.1016/j.heliyon.2020.e04691>)
7. N. A. A. Qasem, R. H. Mohammed, D. U. Lawal, *npj Clean Water* **4** (2021) 36 (<https://doi.org/10.1038/s41545-021-00127-0>)
8. S. Maiti, B. Prasad, A. K. Minocha, *SN Appl. Sci.* **2** (2020) 2151 (<https://doi.org/10.1007/s42452-020-03892-8>)
9. C. I. Orozco, M. S. Freire, D. Gómez-Díaz, J. González-Álvarez, *Sustain. Chem. Pharmacy* **32** (2023) 101016 (<https://doi.org/10.1016/j.scp.2023.101016>)
10. T. Ahmad, M. Danish, M. Dadi, K. Siraj, T. Sundaram, D. S. Raj, S. Majeed, S. Ramasamy, *J. Water Process Eng.* **67** (2024) 106113 (<https://doi.org/10.1016/j.jwpe.2024.106113>)
11. A. M. Elgarahy, K. Z. Elwakeel, S. H. Mohammad, G. A. Elshoubaky, *Cleaner Eng. Technol.* **4** (2021) 100209 (<https://doi.org/10.1016/j.clet.2021.100209>)
12. A. Nurain, P. Sarker, M. S. Rahaman, M. M. Rahman, M. K. Uddin, *J. Multidisc. Appl. Natural Sci.* **1**(2021) 117 (<https://doi.org/10.47352/jmans.v1i2.89>)
13. A. Karnwal, *Desal. Water Treat.* **319**(2024) 100523 (<https://doi.org/10.1016/j.dwt.2024.100523>)
14. U. M. Ismail, M. S. Vohra, S. A. Onaizi, *Environ. Res.* **251** (2024) 118562 (<https://doi.org/10.1016/j.envres.2024.118562>)
15. C. Duan, T. Ma, J. Wang, Y. Zhou, *J. Water Process Eng.* **37** (2020) 101339 (<https://doi.org/10.1016/j.jwpe.2020.101339>)
16. O. A. Ramírez Calderón, O. M. Abdeldayem, A. Pugazhendhi, E. R. Rene, *Current Pollut. Reports* **6** (2020) 8 (<https://doi.org/10.1007/s40726-020-00135-7>)
17. E. Fischer, B. E. N. Kirunda, C. Ewango, M. Leal, D. Kujirakwinja, A. Bamba, A. J. Plumptre, *Phytotaxa* **298** (2017) 277 (<https://doi.org/10.11646/phytotaxa.298.3.7>)
18. R. H. M. Knippers, S. Gallois, T. van Andel, *Economic Botany* **75** (2021) 76 (<https://doi.org/10.1007/s12231-021-09517-4>)
19. M. Danish, R. Hashim, M. N. M. Ibrahim, M. Rafatullah, O. Sulaiman, T. Ahmad, M. Shamsuzzoha, A. Ahmad, *J. Chem. Eng. Data* **56** (2011) 3607 (<https://doi.org/10.1021/je200460n>)
20. A. Chand, P. Chand, G. G. Khatri, D. R. Paudel, *Chem. Biochem. Engineering Quarterly* **35** (2021) 279 (<https://doi.org/10.15255/CABEQ.2021.1943>)
21. S. O. Owalude, A. C. Tella, *Beni-Suef University J. Basic Appl. Sci.* **5** (2016) 377 (<https://doi.org/10.1016/j.bjbas.2016.11.005>)
22. E. Šabanović, M. Memić, J. Sulejmanović, A. Selović, *Polish J. Chem. Technol.* **22** (2020) 46 (<https://doi.org/10.2478/pjct-2020-0007>)
23. N. K. Berber-Villamar, A. R. Netzahuatl-Muñoz, L. Morales-Barrera, G. M. Chávez-Camarillo, C. M. Flores-Ortiz, E. Cristiani-Urbina, *PLOS ONE* **13** (2018) e0196428 (<https://doi.org/10.1371/journal.pone.0196428>)
24. Y. Liu, H. Wang, Y. Cui, N. Chen, *Int. J. Environ. Res. Public Health* **20** (2023) 3885 (<https://doi.org/10.3390/ijerph20053885>)
25. J. Aravind, S. Muthusamy, S. H. Sunderraj, L. Chandran, K. Palanisamy, *Int. J. Indust. Chem.* **4** (2013) 25 (<https://doi.org/10.1186/2228-5547-4-25>)

26. M. M. John, A. Benettayeb, M. Belkacem, C. Ruvimbo Mitchel, M. Hadj Brahim, I. Benettayeb, B. Haddou, S. Al-Farraj, A. A. Alkahtane, S. Ghosh, C. H. Chia, M. Sillanpaa, O. Baigenzhenov, A. Hosseini-Bandegharai, *Chemosphere* **357** (2024) 142051 (<https://doi.org/10.1016/j.chemosphere.2024.142051>)
27. A. A. Alghamdi, A.-B. Al-Odayni, W. S. Saeed, A. Al-Kahtani, F. A. Alharthi, T. Aouak, *Materials* **12** (2019) 2020 (<https://doi.org/10.3390/ma12122020>)
28. H. Urooj, T. Javed, M. B. Taj, M. N. Haider, *Int. J. Environ. Anal. Chem.* **104** (2023) 7474 (<https://doi.org/10.1080/03067319.2023.2176229>)
29. S. Dey, G. T. N. Veerendra, A. V. Phani Manoj, S. S. A. Babu Padavala, *Waste Manag. Bulletin* **2** (2024) 76 (<https://doi.org/10.1016/j.wmb.2024.09.006>)
30. S. U. Khan, F. U. Khan, I. U. Khan, N. Muhammad, S. Badshah, A. Khan, A. Ullah, A. S. Khan, H. Bilal, A. Nasrullah, *Desal. Water Treat.* **57** (2016) 3964 (<https://doi.org/10.1080/19443994.2014.989268>)
31. I. Langmuir, *J. Am. Chem. Soc.* **38** (1916) 2221 (<https://doi.org/10.1021/ja02268a002>)
32. K. Y. Foo, B. H. Hameed, *Chem. Eng. J.* **156** (2010) 2 (<https://doi.org/10.1016/j.cej.2009.09.013>)
33. G. Annadurai, R.-S. Juang, D. Lee, *Water Sci. Technol.* **47** (2003) 185 (<https://doi.org/10.2166/wst.2003.0049>)
34. B. Singha, S. K. Das, *Colloids Surf. B* **107** (2013) 97 (<https://doi.org/10.1016/j.colsurfb.2013.01.060>)
35. M. A. Fawzy, H. M. Al-Yasi, T. M. Galal, R. Z. Hamza, T. G. Abdelkader, E. F. Ali, S. H. A. Hassan, *Sci. Rep.* **12** (2022) 8583 (<https://doi.org/10.1038/s41598-022-12233-1>)
36. N. S. M. Tahiruddin, R. A. Aziz, R. Ali, N. I. Taib, *J. Environ. Chem. Eng.* **11** (2023) 109953 (<https://doi.org/10.1016/j.jece.2023.109953>)
37. J. G. Amrutha, C. R. Girish, B. Prabhu, K. Mayer, *Environ. Process.* **10** (2023) 38 (<https://doi.org/10.1007/s40710-023-00631-0>)
38. M. J. Temkin, V. Pyzhev, *Acta Physicochim. URSS* **12** (1940) 217–225
39. M. M. Dubinin, E. D. Zaverina, L. V. Radushkevich, *Zh. Fiz. Khim.* **21** (1947) 1351
40. M. Polanyi, *Trans. Faraday Soc.* **28** (1932) 316
41. Z. Raji, A. Karim, A. Karam, S. Khalloufi, *Waste* **1** (2023) 775 (<https://doi.org/10.3390/waste1030046>)
42. S. Lagergren, *Kungliga Svenska Vetenskapsakademiens Handlingar.* **24** (1898) 1
43. Y. S. Ho, G. McKay, *Process Biochem.* **34** (1999) 451 ([https://doi.org/10.1016/S0032-9592\(98\)00112-5](https://doi.org/10.1016/S0032-9592(98)00112-5)).